What Triggers NBTI? An "On The Fly" Electron Spin Resonance Approach

J.T. Ryan[1] and P.M. Lenahan[2]
The Pennsylvania State University, University Park, PA 16802
Tel: 814-863-4630, Fax: 814-863-7967, Email: [1]jtr16@psu.edu, [2]pmlesm@engr.psu.edu

T. Grasser[3]
Institute for Microelectronics, Technical University of Vienna, Gusshausstrasse 27-29/E360, 1040 Vienna, Austria
Tel: +43(1)58801-36023, Email: [3]grasser@iue.tuwien.ac.at

H. Enichlmair[4]
austriamicrosystems AG, Schloss Premstaetten, A-8141 Unterpremstaetten, Austria
Tel: +4331365005955, Email: [4]hubert.enichlmair@austriamicrosystems.com

ABSTRACT

We have developed a means to perform "on the fly" electron spin resonance (ESR) measurements of NBTI defect generation. The approach permits ESR measurements to be performed during NBTI stress void of any recovery contamination. We demonstrate that elevated temperature (100°C) and modest negative polarity oxide electric field (<5MV/cm) generates ESR spectra of E' oxide defects. (These defects are holes trapped in oxygen vacancies.) When similar measurements are made at elevated temperature and no oxide bias, E' center spectra are not observed. When ESR measurements are made with identical negative oxide bias at room temperature, E' center spectra are not observed. Furthermore, we demonstrate that the NBTI induced E' center spectrum disappears, a recovery phenomena, when the NBTI stressing condition is removed. These observations indicate that NBTI is triggered by inversion layer hole capture at an E' precursor site (an oxygen vacancy) which then leads to the depassivation of nearby interface states (P_b centers).

INTRODUCTION

The negative bias temperature instability (NBTI) is one of the most important reliability problems facing modern CMOS technology [1-3]. NBTI is manifested as a threshold voltage shift and drive current degradation in pMOSFETs following the application of significant negative bias at elevated temperature. Although the phenomena have being observed for several decades, a fundamental understanding of the physical processes involved in NBTI has yet to be established.

Traditionally, NBTI has been explained in terms of a reaction-diffusion model [1-3]. In the reaction-diffusion model, inversion layer hole capture during NBTI stress leads to hydrogen liberation from passivated interface states [1-3]. The liberated hydrogen diffuses into the gate oxide as an oxide charge leaving unpassivated interface states (P_b centers) at the Si/SiO_2 boundary. The phenomenon of recovery, in which much of the NBTI damage is not permanent, is explained as the reversal of this process [1-3]. When the NBTI stress is removed, hydrogen diffuses back to the Si/SiO_2 interface and repassivates the interface states. Although the reaction-diffusion model generally makes physical sense, many variations of this general idea exist and certain aspects of NBTI are not well explained [1, 2]. A complete picture explaining a wide range of circumstances is not available.

Recent conventional electron spin resonance (ESR) observations of Fujieda et al. [4] and electrically detected magnetic resonance (EDMR) observations of Campbell et al. [5, 6] suggest that NBTI is dominated by Si/SiO_2 interface states (P_b centers) in pure SiO_2 structures. When subject to very severe stress conditions, Campbell et al. also observed E' centers generated [5]. Campbell et al. suggested that E' centers could trigger the NBTI process via an E' center/P_b center hydrogen exchange. This general idea, an E'/P_b center hydrogen exchange triggered by hole capture at an E' site, has been expressed elsewhere [7] and the experimental results of Conley et al. [8, 9] clearly demonstrate that multiple E'/P_b center reactions are thermodynamically and kinetically possible.

Quite recently, Grasser et al. [10] have developed a comprehensive quantitative two stage model for NBTI in which NBTI is triggered by inversion layer hole capture at an E' center precursor site (a neutral oxygen vacancy). The oxide silicon dangling bond created in this process then triggers the creation of poorly recoverable defects (P_b centers). The comprehensive quantitative model of Grasser et al. explains NBTI degradation over a wide range of bias voltage and stress temperature, the observed asymmetry between stress and recovery, and the strong sensitivity to bias and temperature during recovery [10]. Additionally, the model predicts that paramagnetic E' centers will be present during stress, and will very quickly recover upon removal of stress. A schematic illustration of the E' center predicted to be present during NBTI stress is illustrated in figure 1.

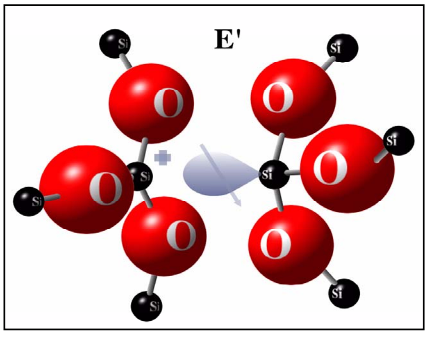

Figure 1: Schematic cartoon illustration of an E' center; a hole trapped in an oxygen vacancy.

Electron spin resonance (ESR) is arguably the most powerful analytical tool available for identifying the atomic scale nature of reliability limiting defects in semiconductor devices [11]. As mentioned previously, Campbell et al. were only able to report

978-1-4244-3922-5/09/$25.00 ©2009 IEEE

somewhat tenuous E' experimental observations in NBTI stress devices [5]. This is so for two reasons. First, and most importantly, the EDMR technique of spin dependent recombination (SDR) does not permit observations at significant negative bias; the stress biasing conditions must be altered so that electron and hole quasi Fermi levels are split more or less symmetrically about the intrinsic Fermi level at the Si/SiO$_2$ interface [11, 12]. Secondly, SDR is only marginally adequate for E' center detection because only those E' centers very close to the interface can contribute to SDR [12]. Conventional ESR does permit E' center detection at any gate bias, if the center is positively charged [11]. In this study, we have developed an "on the fly" approach to magnetic resonance in which ESR measurements are performed during negative bias stressing of MOS structures at elevated temperature. The newly developed approach permits a recovery free glimpse into the dynamics of NBTI.

EXPERIMENTAL

The samples used in this study are simple Si/SiO$_2$ blanket capacitor structures with 49.5nm thermally grown SiO$_2$ oxides. One sample received a forming gas anneal, the other sample did not. ESR measurements were done before, during, and after the samples were subjected to a negative bias (-25V) temperature stress (100°C). Negative bias was applied to the samples utilizing corona discharge [13] and the gate bias was monitored before and after stress with a Kelvin probe. Elevated temperature was provided by outfitting the spectrometer with a cryogenic cold finger system modified to heat the sample under study. ESR measurements were made on a commercially available Bruker Instruments X-band spectrometer with a TE$_{104}$ microwave cavity. The ESR measurements were calibrated using a weak pitch spin standard.

RESULTS AND DISCUSSION

Figure 2 illustrates pre-stress ESR spectra for both the forming gas (bottom) and no forming gas (top) samples at identical spectrometer gain. The sample which did not receive the forming gas (top) displays three spectra with g = 2.0063 (P$_{b0}$ Si/SiO$_2$ interface states), g = 2.0036 (P$_{b1}$ Si/SiO$_2$ interface states), and g = 2.0006 (E' oxide defects). (The g is defined a $g = h\nu/\beta H$, where h is Planck's constant, ν is the microwave frequency, β is the Bohr magneton, and H is the magnetic field at resonance. The g depends on the defect's structure and its orientation with respect to the applied magnetic field; it is essentially a second rank tensor [14].) The sample which did receive the forming gas anneal (bottom) displays a much weaker signal with g = 2.0069 which is consistent with a low density of Si/SiO$_2$ P$_{b0}$ centers. The second integral of the ESR signal is proportional to the number of defects present. As expected, the forming gas annealed sample has far fewer defects present pre-stress.

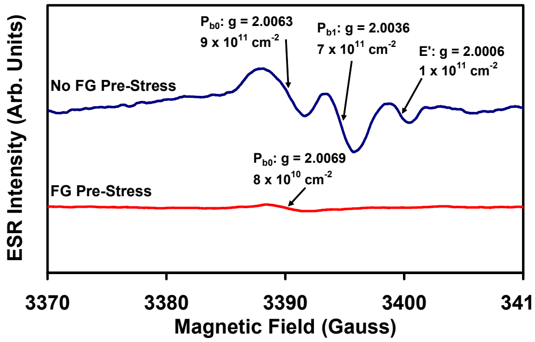

Figure 2: Comparison of pre-stress ESR spectra plotted with identical spectrometer gain for the sample without forming gas (top trace) and the sample with forming gas (bottom trace).

Figures 3 and 4 each illustrate three ESR traces taken at room temperature for the sample without forming gas (figure 3) and with forming gas (figure 4). The top traces were taken on the as processed samples, the middle traces were taken with the samples biased with -25V at room temperature, and the bottom traces taken after removing the bias. The room temperature corona bias of -25V does not result in an increase of interface states (P$_b$ centers) or oxide defects (E' centers) in either the no forming gas sample (figure 3) or forming gas sample (figure 4). It does, of course, suppress the P$_{b0}$ and P$_{b1}$ signals because these defects are interface traps [15].

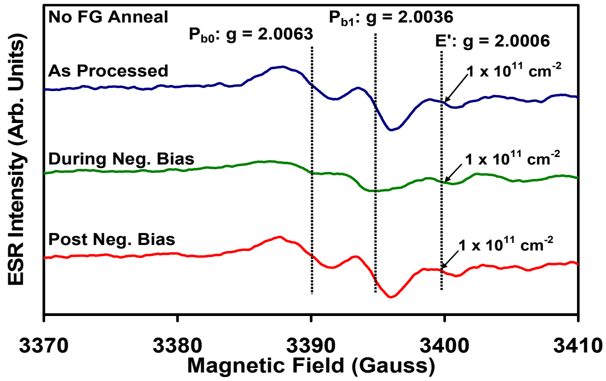

Figure 3: Room temperature ESR traces taken on the sample which did not receive a forming gas anneal as processed (top trace), with -25V bias (middle trace), and after removal of negative bias (bottom trace). Note that the negative bias alone does not generate additional E' defects (or P$_b$ interface states) in this sample.

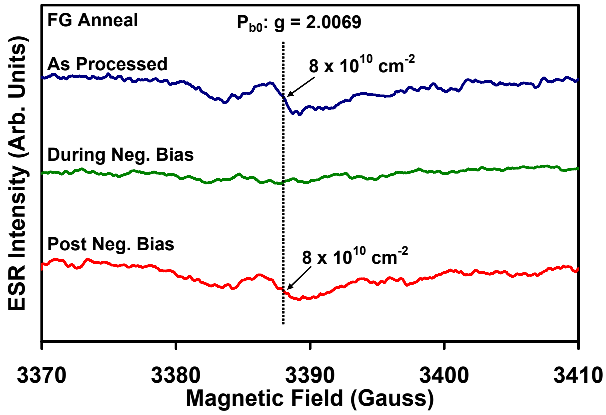

Figure 4: Room temperature ESR traces taken on the sample which did receive a forming gas anneal as processed (top trace), with -25V bias (middle trace), and after removal of negative bias (bottom trace). Note that the negative bias alone does not generate additional E' defects (or P$_b$ interface states) in this sample.

Figures 5 and 6 each illustrate three ESR traces taken before, during and after NBTI stress for the sample without forming gas (figure 5) and with forming gas (figure 6). The spectrometer settings used in all cases were chosen to permit the observation of both Si/SiO$_2$ P$_b$ centers and SiO$_2$ E' centers and are not optimized for either defect; the E' center density is underrepresented in these traces. (There is a significant difference in E' and P$_b$ spin lattice relaxation times which leads to this underrepresentation [16].)

Figure 5 illustrates three ESR traces taken on the sample not treated with forming gas. As mentioned previously, in the pre-stress case (top trace) we observe three spectra which are consistent with P$_{b0}$ centers (g = 2.0063), P$_{b1}$ centers (g = 2.0036), and E' centers (g =

2.0006). During NBTI stress (middle trace) we observe a clear increase in the second integral of the E' signal. This corresponds to an increase of about a factor of four in positively charged E' sites. Upon removal of the stress conditions (bottom trace) the E' signal second integral returns to its original pre-stress value. The result clearly demonstrates that E' centers are generated during NBTI stress and very quickly recover upon removal of the stress; that is, positively charged oxygen vacancy sites are generated during stress and very quickly recover.

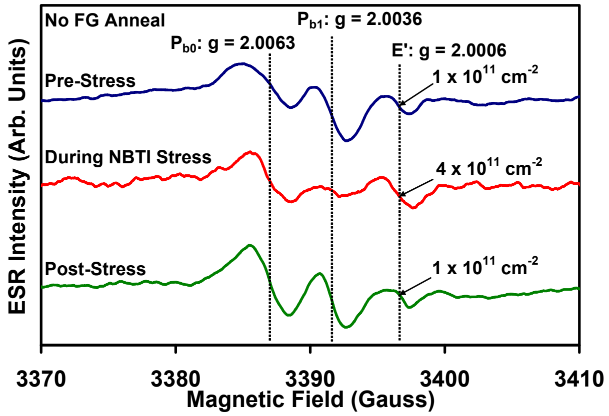

Figure 5: Three ESR traces for the sample which did not receive a forming gas anneal. Note the clear increase in the E' signal intensity during NBTI stressing (middle) and their subsequent recovery post-stress (bottom).

Figure 6 illustrates three ESR traces taken on the sample that was treated with forming gas. As mentioned previously, in the pre-stress case (top trace), we observe a weak single line spectrum with g = 2.0069 due to P_{b0} interface states. During NBTI stress, we observe the generation of Si/SiO_2 P_{b1} centers (g = 2.0034) and SiO_2 E' centers (2.0006). Upon removal of the stress, the g = 2.0006 E' center signal completely recovers while some of the P_{b1} centers remain. Again, this result clearly demonstrates that positively charged oxygen vacancy sites (E') centers are generated during stress and recover once the stress is removed.

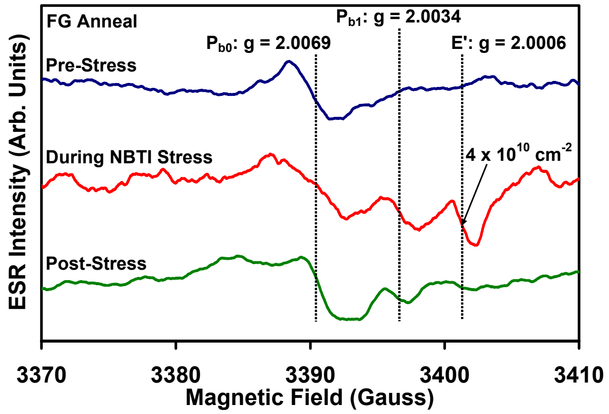

Figure 6: Three ESR traces for the sample which did receive the forming gas anneal. Note the clear generation of an E' signal during NBTI stress (middle), as well as P_{b1} center generation, and the nearly complete recovery of the E' defects post-stress (bottom).

As mentioned previously, the spectrometer settings used in figures 2-6 were chosen to permit the observation of both Si/SiO_2 P_b centers and SiO_2 E' centers and are not optimized for either defect.

In an attempt to further demonstrate that E' centers (positively charged oxygen vacancy sites) are present during NBTI stressing, figure 7 shows three ESR traces taken on the sample which did receive forming gas before, during and after NBTI stressing. In this figure, the spectrometer settings are optimized for the observation of E' centers. When NBTI stressing is applied, a clear signal with $g_{\parallel}$=2.0016 and $g_{\perp}$ = 2.0006 appears which is characteristic of an E' center. Upon removal of the NBTI stress, the E' signal completely recovers. Figure 8 further demonstrates the identification of this signal as due to an E' center by comparing the during NBTI stress spectra of figure 7 with that of a commercially available E' standard [17]. Note the close correspondence between the g values and the line shapes which are characteristic to this type of defect.

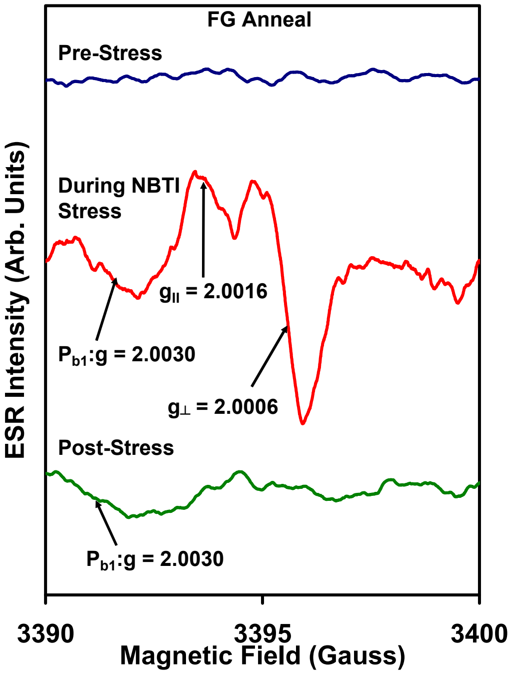

Figure 7: Three ESR traces taken on the sample which received the forming gas anneal. In these traces, the spectrometer settings are optimized to observe E' centers. Note the clear generation of an E' spectrum during stress and its subsequent recovery post-stress.

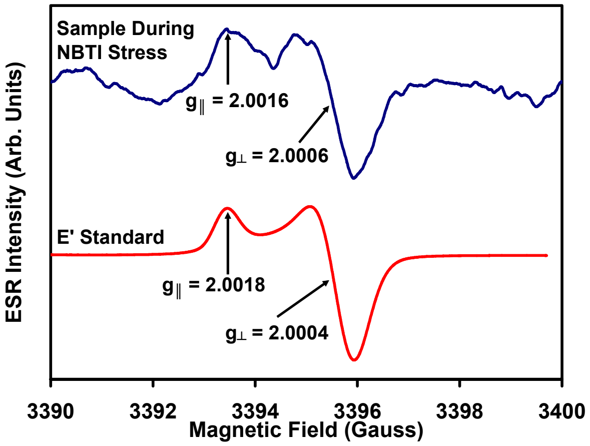

Figure 8: Comparison of the forming gas annealed sample during NBTI stress from figure 7 (top) and a commercially available E' standard. The standard sample signal to noise is much higher because the standard has orders of magnitude more E' centers. Note the close correspondence between the g values and line shapes. The gain of the sample trace is approximately 10,000 times larger that

used for the E’ standard; all other spectrometer settings are identical. (Note that the precision of g is ±0.0002.)

CONCLUSIONS

These observations are consistent with and most strongly support the suggestions of Campbell et al. [5] and Grasser et al. [10] that NBTI is triggered by the tunneling of electrons from a neutral E’ center precursor to unoccupied valence band states. The results of this study are also consistent with and supports the comprehensive NBTI model recently proposed by Grasser et al. [10] Work at Penn State supported by Texas Instruments through SRC Custom Funding. Part of this work has received funding from the European Community’s Seventh Framework Programme under Grant Agreement No. 216436 (project ATHENIS).

REFERENCES

[1] T. Grasser, W. Goes, and B. Kaczer, “Toward engineering modeling of negative bias temperature instability,” in Defects in microelectronic materials and devices, D.M. Fleetwood, S.T. Pantelides, and R.D. Schrimpf. Boca Raton, London, New York: CRC Press, 2009, pp. 399-436.

[2] G. LaRosa, “Negative bias temperature instabilities in pMOSFET devices,” in IEEE Series on Microelectronic Systems, A.W. Strong, E.Y. Wu, R.P. Vollertsen, J. Sune, G. LaRosa, S.E. Rauch, and R.P. Sullivan. Hoboken: Wiley, 2009, pp. 331-439.

[3] D.K. Schroder and J.A. Babcock, “NBTI: Road to cross in deep submicron Si semiconductor manufacturing,” *J. Appl. Phys.*, **94**, pp. 1-18 (2003).

[4] S. Fujieda, Y. Miura, M. Saitoh, E. Hasegawa, S. Koyama, and K. Ando, “Interface defects responsible for NBTI in plasma-nitrided SiON/Si(100) systems,” *Appl. Phys. Lett.*, **82**, pp. 3677-3679 (2003).

[5] J.P. Campbell, P.M. Lenahan, A.T. Krishnan, and S. Krishnan, “Observations of NBTI-induced atomic-scale defects,” *IEEE Trans. Dev. Mater. Reliab.*, **6**, pp. 117-122 (2006).

[6] J.P. Campbell, P.M. Lenahan, A.T. Krishnan, and S. Krishnan, “Direct observation of the structure of defect centers involved in the negative bias temperature instability,” *Appl. Phys. Lett.*, **87**, pp. 204106 (2005).

[7] P.M. Lenahan, “Atomic scale defects involved in MOS reliability problems,” *Microelectron. Eng.*, **69**, pp. 173-181 (2003).

[8] J.F. Conley, P.M. Lenahan, A. Lelis, and T.R. Oldham, “Electron spin resonance evidence for the structure of a switching oxide trap: long term structural change at silicon dangling bond sites in SiO_2,” *Appl. Phys. Lett.*, **67**, pp. 2179-2181 (1995).

[9] J.F. Conley, P.M. Lenahan, A.J. Lelis, and T.R. Oldham, “Electron spin resonance evidence that E’(gamma) centers can behave as switching oxide traps,” *IEEE Trans. Nucl. Sci.*, **42**, pp. 1744-1749 (1995).

[10] T. Grasser, B. Kaczer, W. Goes, T. Aichinger, P. Hehenberger, and M. Nelhiebel, “A two-stage model for negative bias temperature instability,” *Proc. IEEE Intl. Reliab. Phys. Symp.*, pp. 33-44 (2009).

[11] P.M. Lenahan and J.F. Conley, “What can electron paramagnetic resonance tell us about the Si/SiO_2 system?” *J. Vac. Sci. Technol., B*, **16**, pp. 2134-2153 (1998).

[12] P.M. Lenahan and M.A. Jupina, “Spin dependent recombination at the Si/SiO_2 interface,” *Colloids Surf.*, **45**, pp. 191-211 (1990).

[13] M.S. Dautrich, P.M. Lenahan, A.Y. Kang, and J.F. Conley, “Noninvasive nature of corona charging on thermal Si/SiO_2 structures,” *Appl. Phys. Lett.*, **85**, pp. 1844-1845 (2004).

[14] J.A. Weil, J.R. Bolton, and J.E. Wertz, “Electron Paramagnetic Resonance”. New York, NY: Wiley, 1994.

[15] J.P. Campbell and P.M. Lenahan, “Density of states of P_{b1} Si/SiO_2 interface trap centers,” *Appl. Phys. Lett.*, **80**, pp. 1945-1947 (2002).

[16] P.M. Lenahan and P.V. Dressendorfer, “Hole traps and trivalent silicon centers in metal-oxide silicon devices,” *J. Appl. Phys.*, **55**, pp. 3495-3499 (1984).

[17] E’ standard available from Wilmad Lab Glass.

QUESTIONS AND ANSWERS

Q1: What is the duration of the stress?

A1: The OTF-ESR technique is not fast by any means; it takes about 6-8 hours for me to acquire a decent looking spectrum during stress.

Q2: Is there any interface trap recovery in the experiment?

A2: Remember that it is difficult to obtain a good density of interface states during the stress because we have rendered some of the interface states diamagnetic. Also, these measurements take a long time to run so our time resolution is not that great. I don’t think I can give definitive yes or no because of the limitations of the measurement.

Q3: Have you done any PBTI stressing?

A3: We have preliminary data where we PBTI stress the samples and we do not see E’ centers being generated. We only see the E’ centers show up with the combination of negative bias and elevated temperature